Cell Research (2007) 17:858-868.

www.nature.com/cr

ORIGINAL ARTICLE

Rig-I$^{-/-}$ mice develop colitis associated with downregulation of Gαi2

Yi Wang[1*], Hong-Xin Zhang[1*], Yue-Ping Sun[1], Zi-Xing Liu[1], Xue-Song Liu[1], Long Wang[2,3], Shun-Yuan Lu[2,3], Hui Kong[3], Qiao-Ling Liu[3], Xi-Hua Li[1], Zhen-Yu Lu[1], Sai-Juan Chen[2], Zhu Chen[2], Shi-San Bao[4], Wei Dai[5], Zhu-Gang Wang[1,2,3,4]

[1]Department of Medical Genetics, Shanghai Jiao Tong University School of Medicine, Shanghai 200025, China; [2]State Key Laboratory of Medical Genomics, Rui-Jin Hospital Affiliated to Shanghai Jiao Tong University School of Medicine, Shanghai 200025, China; [3]Shanghai Research Center for Model Organisms, Shanghai 201203, China; [4]Department of Pathology, University of Sydney, Sydney, 2570 NSW, Australia; [5]Department of Environmental Medicine, New York University School of Medicine, Tuxedo, NY 10987, USA

RIG-I (retinoid acid-inducible gene-I), a putative RNA helicase with a cytoplasmic caspase-recruitment domain (CARD), was identified as a pattern-recognition receptor (PRR) that mediates antiviral immunity by inducing type I interferon production. To further study the biological function of RIG-I, we generated *Rig-I*$^{-/-}$ mice through homologous recombination, taking a different strategy to the previously reported strategy. Our *Rig-I*$^{-/-}$ mice are viable and fertile. Histological analysis shows that *Rig-I*$^{-/-}$ mice develop a colitis-like phenotype and increased susceptibility to dextran sulfate sodium-induced colitis. Accordingly, the size and number of Peyer's patches dramatically decreased in mutant mice. The peripheral T-cell subsets in mutant mice are characterized by an increase in effector T cells and a decrease in naïve T cells, indicating an important role for Rig-I in the regulation of T-cell activation. It was further found that *Rig-I* deficiency leads to the downregulation of G protein αi2 subunit (Gαi2) in various tissues, including T and B lymphocytes. By contrast, upregulation of *Rig-I* in NB4 cells that are treated with ATRA is accompanied by elevated *Gαi2* expression. Moreover, *Gαi2* promoter activity is increased in co-transfected NIH3T3 cells in a Rig-I dose-dependent manner. All these findings suggest that Rig-I has crucial roles in the regulation of *Gαi2* expression and T-cell activation. The development of colitis may be, at least in part, associated with downregulation of *Gαi2* and disturbed T-cell homeostasis.

Keywords: *Rig-I* knockout mice, colitis, Peyer's patches, T-cell homeostasis, *Gαi2* expression

Cell Research (2007) **17**:858-868. doi: 10.1038/cr.2007.81; published online 25 September 2007

Introduction

RIG-I (retinoid acid-inducible gene-I) was originally found to be upregulated in differentiating NB4 cells that are induced by all-trans retinoic acid (ATRA) [1, 2]. It is a member of the DExD/H box protein family containing a C-terminal helicase domain and two tandem caspase-recruitment domains (CARDs) [3]. Recent studies have shown that RIG-I plays a crucial part in guarding against viral invasion as an intracellular molecular sensor. RIG-I binds to synthetic dsRNA or viral dsRNA through its helicase domain, inducing a conformational change that allows the N-terminal CARD domains to recruit the downstream signaling protein MAVS (also called IPS-1, VISA, and Cardif). The interaction between RIG-I and MAVS triggers both NF-κB and IRF3 signaling pathways, leading to the activation of the IKK and TBK-1/IKKε kinase complexes, and, subsequently, the induction of IFN-β. Hepatitis C virus (HCV) can interrupt RIG-I signaling to IRF-3 and NF-κB through the cleavage of MAVS by its NS3/4 protease [4-11]. The RIG-I-mediated antiviral activity is negatively

*These authors contributed equally to this work.
Correspondence: Zhu-Gang Wang
Tel/Fax: +86-21-6445799
E-mail: zhugangw@shsmu.edu.cn
Received 22 January 2007; revised 1 April 2007; accepted 9 May 2007; published online 25 September 2007

regulated by the A20 protein [12]. It has been shown that RIG-I, but not the TLR system, has an essential role in the antiviral response *in vivo* in various cells except pDCs [13]. Thus, RIG-I is thought to be the third pattern-recognition receptor in addition to TLRs and NLRs. Moreover, RIG-I can also regulate the transcription of many genes including interferon-γ stimulated gene 15 in MCF-7 cells and *COX-2* in endothelial cells [14,15].

Human inflammatory bowel disease (IBD), including Crohn's disease and ulcerative colitis, is a multifactor disease that is manifested by cellular inflammation and intestinal tissue damage. It is also characterized by the dysfunction of mucosal immunity, including the malfunction of T cells and aberrant cytokine production. However, the precise mechanism that underlies colitis remains unclear. Studies on mice with targeted disruption of the genes that regulate the T-cell immune responses have shed light on the development of colitis. For example, mice with targeted disruption of *Gαi2* develop colitis with 100% penetrance [16, 17]. *Gαi2* is regarded as one of the candidate genes for IBD in human, because genetic linkage studies have mapped the *Gαi2* gene within an IBD susceptible locus at chromosome 3p21 [18]. Heterotrimeric G proteins consist of α, β and γ subunits. *Gαi2* is one of the *Gα* subunits, which has a role in a large variety of cellular and metabolic processes [19-23]. Furthermore, a decreased number of Peyer's patches was also observed in *Gαi2*$^{-/-}$ mice [16,17,19]. It is important to emphasize that Peyer's patches provide the first line of defense against pathogen invasion in the intestine. Mice with *Gαi2* ablation exhibit an accelerated transition from double-positive to single-positive thymocytes, leading to selective CD4^{+} T-cell disorders. Increases in effector T cells and decreases in naïve T cells were also observed in the spleen of *Gαi2*$^{-/-}$ mice [24,25]. These data suggest that *Gαi2* is associated with the induction of colitis and that it is a negative regulator of the T-cell response.

To further investigate the biological function of RIG-I, we generated *Rig-I*-deficient (*Rig-I*$^{-/-}$) mice through homologous recombination, taking a different strategy to the previously reported strategy [13]. We found that *Rig-I*$^{-/-}$ mice are viable and fertile. They develop a colitis-like phenotype and increased susceptibility to dextran sulfate sodium (DSS)-induced colitis, which is accompanied by a decrease in the size and number of Peyer's patches, abnormal activation of peripheral T cells and downregulation of *Gαi2*. These findings reveal a novel role for Rig-I in the regulation of intestinal mucosal immunity and *Gαi2* expression.

Materials and Methods

Generation of Rig-I knockout mice

A *Rig-I* targeting vector was designed to delete the 6.4-kb fragment that contains exons 4 to 8, which encodes part of the CARD domain 2, and that contains the A and B motifs of the RNA helicase domain. The targeting construct was electroporated into ES cells. After double selection with G418 and GANC, the resistant clones were genotyped using Southern blotting. Two correctly recombined ES cell clones were used to create *Rig-I* mutant mice through blastocyst microinjection. The *Rig-I*$^{+/-}$ mice were generated by crossing chimeras with wild-type 129S1 mice. They were genotyped by PCR using two primer pairs in one reaction, which allows the amplification of wild type and targeted alleles. The primers used for genotyping were 5′-GCCTAGCTAGCCAAAGTAACAC-3′ and 5′-GCAGCGCATCGCCTTCTATC-3′ for the targeted allele, and 5′-CACAGTTGCCTGCTGCTCAT-3′ and 5′-CAGGAAGAGCCAGAGTGTCAGAAT-3′ for the wild-type allele. PCR was run for 30 cycles at 94 °C for 30 s, 58 °C for 90 s, 72 °C for 90 s, and a final extension at 72 °C for 10 min after an initial denaturation at 94 °C for 5 min. The *Rig-I* mutant mice were bred in specific pathogen-free conditions and maintained in a 129S1 background.

Northern blot analysis

Mouse primary embryonic fibroblasts (MEFs) were isolated from 13.5 dpc embryos and plated at a concentration of 2×10^6 cells in 10-cm dishes. The cells were treated with 1000 U/ml murine IFN-β for 24 h. Total RNA was extracted using the TRIZOL reagent (Invitrogen, Carlsbad, CA, USA) and analyzed with northern blotting, using a 477-bp *Rig-I* cDNA fragment (477 bp, composed of exons 11 to 14) as a probe.

Western blot analysis

Cell suspensions from the spleen were prepared by passing tissues through a cell strainer. 10^6 splenocytes were stimulated by LPS (20 μg/ml) for 72 h. Cell lysates were prepared by adding 0.6 ml of RIPA buffer (1% Nonidet P-40, 0.5% sodium deoxycholate, 0.1% SDS in PBS) with freshly supplemented protease inhibitors (100 μg/ml PMSF, 50 KIU/ml aprotinin, 1 mM sodium orthovanadate). In addition, cell lysates were also prepared from the colons and intestines of mice at 8 weeks of age as described above. Cell lysates (50 μg) from cells or tissues were electrophoresed and transferred to PVDF membrane (BioRad, Hercules, CA, USA) according to the manufacturer's protocol. The protein blots were blocked with 5% non-fat milk in TBS, then incubated overnight with antibodies to RIG-I (1:2000 dilution in the blocking buffer), to Gαi2 (1:1000) (Santa Cruz Biotechnology, Inc. CA, USA), or to α-tubulin (1:10 000) (KPL, Gaithersburg, MD, USA). After washing, the membrane was incubated with horseradish peroxidase (HRP) conjugated anti-rabbit IgG (1:10 000, Sigma Chemical Co., St Louis, MO, USA). The blots were immersed in chemiluminescence luminol reagent (Pierce Chemical Co., Rockford, IL, USA) and exposed to X-ray film (Eastman Kodak, Rochester, NY, USA).

Histological assessment of colitis

Colons of wild type and *Rig-I*$^{-/-}$ mice at 8 weeks of age were collected and fixed with 10% formalin for sectioning, followed by hematoxylin-and-eosin staining. Histological assessment was performed in a double-blind fashion. In brief, scores were determined as follows [26-28]: 0, normal morphology; 1, focal inflammatory cell infiltrate around the crypt base; 2, diffuse infiltration of inflammatory cells around the crypts or erosion/destruction of the lower one-third of the glands; 3, erosion/destruction of the lower two-thirds of the glands or loss of all the glands but with the surface epithelium

remaining; and 4, loss of all the glands and epithelium. Each field was assigned a grade of 0 to 4.

Induction and assessment of DSS-induced colitis

Wild type and *Rig-I*$^{-/-}$ mice at 8 weeks of age were divided into two groups, receiving either water alone (control) or 3% (w/v) DSS (40 000–50 000 MW; Sigma Chemical Co., St Louis, MO, USA) in water for 5 days. The mice were checked each day for the development of colitis by monitoring their body weight and diarrhea. The degree of diarrhea was scored as follows: 0, normal; 2, loose stool; and 4, watery diarrhea [29, 30]. All mice were sacrificed after the experiment and the colons were taken for histological analysis. The methods and histological scores used were same as described above.

Analysis of apoptosis

Peyer's patches were collected from wild type and *Rig-I*$^{-/-}$ mice and fixed in 10% neutral buffered formalin. Paraffin-embedded Peyer's patches were sectioned at 5 μm and apoptosis was investigated using the *in situ* TUNEL assay kit (Promega Co., Madison, WI, USA) according to the manufacturer's instructions. Apoptosis was also analyzed by flow cytometry. Peyer's patches were washed three times in cold PBS, and cell suspensions were obtained by passing tissue through a 200-μm nylon mesh. The Peyer's patch lymphocytes (1×10^6) were stained with Annexin-V-FITC (Becton Dickinson, San Jose, CA, USA), PI and B220-APC (Becton Dickinson Immunocytometry, San Jose, CA, USA) antibodies for 30 min at 4°C. The analysis was performed on a FACSCalibur machine (Becton Dickinson, Franklin Lakes, NJ, USA) and the data obtained were processed with CellQuest software (Becton Dickinson, San Jose, CA, USA).

Analysis of T-cell subsets

Splenic lymphocytes from wild type and *Rig-I*$^{-/-}$ mice were obtained by passing tissue through a 200-μm nylon mesh. Erythrocytes were lysed using a lysis buffer. Cells were counted and stained with fluorochrome-conjugated antibodies specific for CD4, CD8, CD44 and CD62L (eBioscience, San Diego, CA, USA) for 30 min. Flow cytometry analysis was performed as described above.

Semi-quantitative RT-PCR and real-time PCR

Total RNA was extracted with the Trizol reagent (Invitrogen, Carlsbad, CA, USA) according to the manufacturer's protocol. For semi-quantitative RT-PCR and real-time PCR, RNA was treated with RNase-free DNase, and then 1 μg total RNA was reverse-transcribed according to the standard protocol (TaKaRa Shuzo, Ltd, Kyoto). The primers used were as follows: 5′-TTGGCCGCTCACGAGAATA-3′ and 5′-GCTGACCACCCACATCAAACA-3′ for *Gαi2*; 5′-TCTTTGCTGACCTGCTGGATT-3′ and 5′-TTCGAGAGGTCCTTTTCACCA-3′ for *HPRT*; and 5′-AACGAGCGGTTCCGATGCCCTGAG-3′ and 5′-TGTCGCCTTCACCGTTCCAGTT-3′ for β-*actin*. Semi-quantitative RT-PCR consists of 25-30 cycles at 94 °C for 30 s, 58 °C for 30 s, 72 °C for 30 s and a final extension at 72 °C for 10 min after an initial denaturation at 94°C for 5 min. Real-time PCR was performed using an ABI9700 PCR machine (Applied Biosystems, Foster City, CA, USA) for 40 cycles at 94 °C for 15 s, 58 °C for 15 s, 72 °C for 30 s and a final extension at 72 °C for 10 min after an initial denaturation at 94 °C for 5 min.

Purification of T cells and B cells from the spleen

Splenocytes of wild type and *Rig-I*$^{-/-}$ mice were collected as described above. Splenic T cells labeled with CD3-PE were sorted out with a MoFlo high-speed cell sorter (DakoCytomation, Denmark). Splenic B cells were isolated using a Dynabeads® Mouse pan B (B220) (Dynal Biotech, Lake Success, NY, USA).

NB4 cell culture and treatment with ATRA

Retinoid acid-sensitive NB4 cells were cultured in RPMI 1640 medium (GIBCO, Grand Island, NY, USA), containing 10% FCS, 100 μg/ml streptomycin and 100 U/ml penicillin in an incubator at 37 °C. The cells were treated with 1 μM ATRA for 0, 24, 48 and 72 h, then the cells were lysed and total RNA was extracted for semi-quantitative RT-PCR.

Construction of pGL3-Gαi2 and pcDNA3.1-Rig-I

A 1.2-kb fragment of mouse *Gαi2* promoter was isolated from mouse genomic DNA by PCR using 5′-AGCCATCCCTCCCGCCCCCCATTT-3′ as the forward primer and 5′-TCTCAGGTCCGCAGTTCCGAGCGA-3′ as the reverse primer. The PCR product obtained was cloned into pGL3-Basic (Promega Co., Madison, WI, USA), using the *Xho*I and *Sac*I sites. Full-length *Rig-I* cDNA was also amplified by PCR using the forward primer 5′-ACTGCGGCCGCCCCACTTCGTTCATCTCTG-3′ and the reverse primer 5′-ACTGGGTACCACGGACATTTCTGCAGGATC-3′. The PCR product was sequenced and cloned to pcDNA3.1 at the *Not*I and *Kpn*I sites. PCR amplification conditions consisted of 30 cycles at 94 °C for 30 s, 60 °C for 90 s, 68 °C for 180 s and a final extension at 72 °C for 10 min after an initial denaturation at 94 °C for 5 min. The construction was sequenced to verify that the proper sequence was amplified.

Luciferase assay

NIH3T3 cells were seeded at a concentration of 8×10^4/ml in 12-well plates. The cells were co-transfected with the *Gαi2* luciferase reporter construct (300 ng), *Renilla* luciferase and pcDNA3.1-*Rig-I* with increasing amounts (0, 300, 500 and 700 ng), or pcDNA3.1 (to keep the total amount of plasmids constant) using the SuperFect Transfection Reagent (Qiagen GmbH, Germany). In a standard assay, each transfection was tested in duplicate according to the protocol of the dual-luciferase reporter assay system kit (Promega Co., Madison, WI, USA).

Statistical analysis

In vivo experiments were performed using 5-10 mice per group. Each *in vitro* experiment was performed in triplicate and repeated three times. All values were expressed as the mean ± SD. Student's two-tailed *t*-test was used to analyze the significance among different groups. A *p*-value of less than 0.05 was considered to be significant and is shown by an asterisk.

Results

Targeted disruption of Rig-I

Intracellular viral infection is detected by the cytoplasmic RNA helicase RIG-I, which highlights a novel role for CARD-containing proteins in coordinating immune and apoptotic responses [31-34]. To further investigate the func-

tion of RIG-I, we disrupted 5 (4 to 8 exons) out of 18 exons of the *Rig-I* gene. In the mutant allele, exons 4 to 8 were replaced by the neo cassette (Figure 1A). G418 and GANC double resistant ES clones were examined for recombination by PCR. The correctly recombined ES clones were further confirmed by Southern blotting (Figure 1B). Two targeted ES clones were identified. Mice with wild type and the targeted allele were identified using PCR, which exhibited different bands of 1.58 kb (wild-type allele) and 2.84 kb (knockout allele) (Figure 1C). The disruption of Rig-I was confirmed by northern blotting with a *Rig-I* probe (Figure 1D) and western blotting using a polyclonal antibody to Rig-I (Figure 1E), respectively. It was found that Rig-I can be induced by IFNβ and LPS in various tissues and cell types [15,35], as shown in wild-type MEFs treated with IFNβ and splenocytes treated with LPS (Figure 1D and 1E). By contrast, no signals were detected by northern and western blotting in *Rig-I*$^{-/-}$ MEFs and splenocytes even

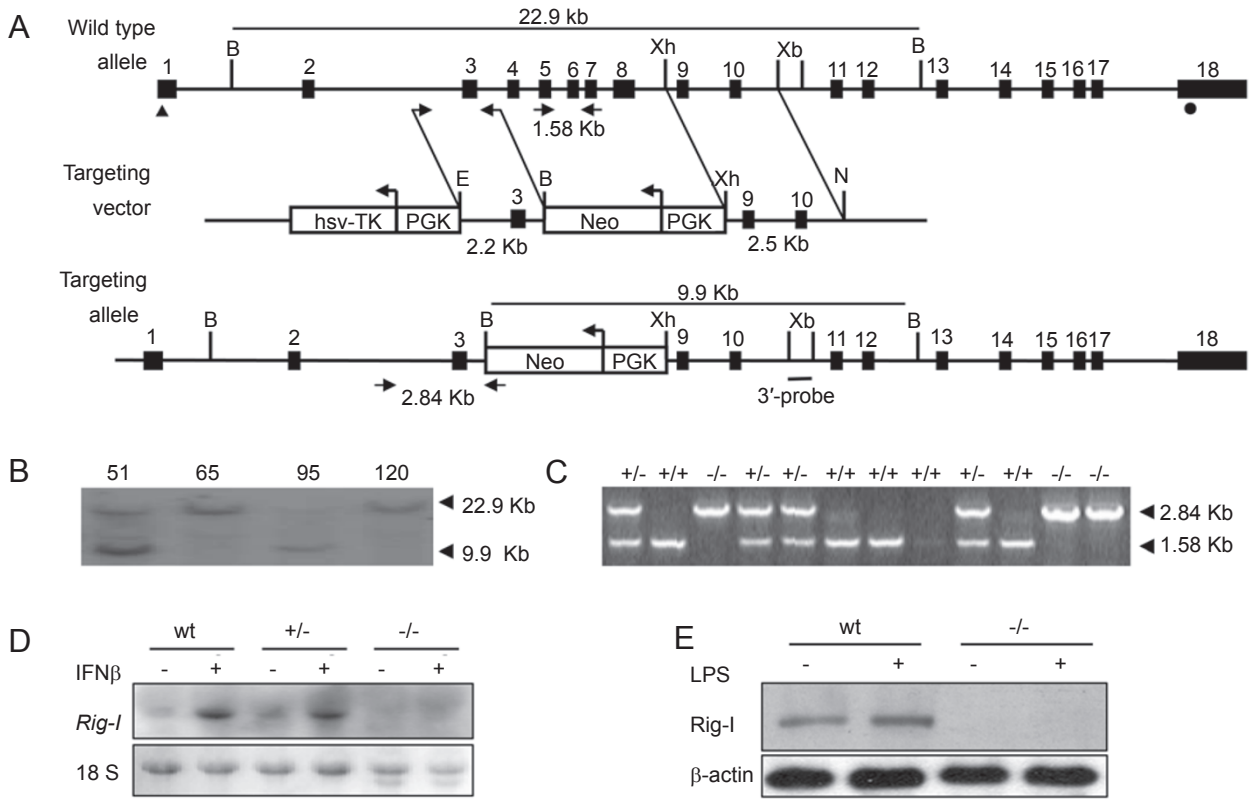

Figure 1 Targeted disruption of *Rig-I*. **(A)** *Rig-I* targeting strategy. Mouse genomic *Rig-I* contains 18 exons. The start codon and stop codon are indicated as ▲ and ●, respectively. The targeting vector was designed to delete a 6.4-kb fragment containing exons 4 to 8, which encode part of CARD domain 2, and containing the A and B motifs of the RNA helicase domain. The 3′ probe used for southern blotting (—) and two primer pairs (arrows) for PCR genotyping are indicated. The respective sizes of the wild type and targeted bands hybridized with the 3′ probe in southern blotting upon *Bam*HI (shown as **B**) digestion, and of the PCR fragments amplified from wild type and mutant alleles are indicated. **(B)** Two recombined ES cell clones show the expected bands as detected by Southern blot analysis. **(C)** PCR using mouse tail DNA as a template and two primer pairs in one reaction shows three different genotypes. **(D)** Northern blot analysis of *Rig-I* in MEFs. Total RNA from wild type, *Rig-I*$^{+/-}$ and *Rig-I*$^{-/-}$ MEFs treated with or without 1000 U/ml IFN-β for 6 h was extracted and subjected to northern blot analysis using an *Hin*dIII fragment of *Rig-I* cDNA (477 bp, composed of exons 11 to 14). The same membrane was re-hybridized with an 18S probe as a control. Note that no signal was detected in *Rig-I*$^{-/-}$ MEFs with or without treatment with IFN-β. **(E)** Western blot analysis of Rig-I expression in wild type and *Rig-I*$^{-/-}$ splenocytes with or without treatment with LPS (20 μg/ml) was performed using the polyclonal antibody raised in mice by immunizing mice with a glutathione S-transferase (GST)-RIG-I fusion protein encompassing the full-length human RIG-I. The same membrane was blotted again with antibody to β-actin. As reported by others, Rig-I can be induced by LPS in various tissues as well as splenocytes, while no bands were visualized in *Rig-I*$^{-/-}$ splenocytes even after treatment with LPS.

after IFNβ and LPS treatment, respectively. The mutant mice develop normally and they are fertile.

Rig-I$^{-/-}$ mice develop colitis with increased susceptibility to DSS-induced colitis

It was observed that the body weight of *Rig-I$^{-/-}$* mice progressively decreased from 3 months of age on compared with that of the wild type (data not shown). *Rig-I$^{-/-}$* mice at 8 weeks of age displayed a colitis-like phenotype (Figure 2A); the incidence was around 70% (data not shown). After treatment with DSS, *Rig-I$^{-/-}$* mice exhibited more severe damage and inflammatory infiltration in the mucosa of the colon than was observed in wild-type mice (Figure 2A). The histological scores were significantly increased in *Rig-I$^{-/-}$* mice (Figure 2B). More body weight loss and higher faecal scores were also observed in *Rig-I$^{-/-}$* mice after DSS treatment (Figure 2C and 2D). These findings indicate that *Rig-I$^{-/-}$* mice are much more susceptible to DSS-induced colitis than wild-type mice.

Decrease in number and size of Peyer's patches in Rig-I$^{-/-}$ mice

Since the disruption of Rig-I in mice leads to the development of a colitis-like phenotype and increased susceptibility to DSS-induced colitis, and the development of colitis in *Gαi2$^{-/-}$* mice is accompanied by fewer Peyer's patches, we also checked the number and size of Peyer's patches in *Rig-I$^{-/-}$* mice. It was found that the number and size of Peyer's patches were significantly reduced in *Rig-I$^{-/-}$* mice compared with wild-type mice (Figure 3A and 3B). The

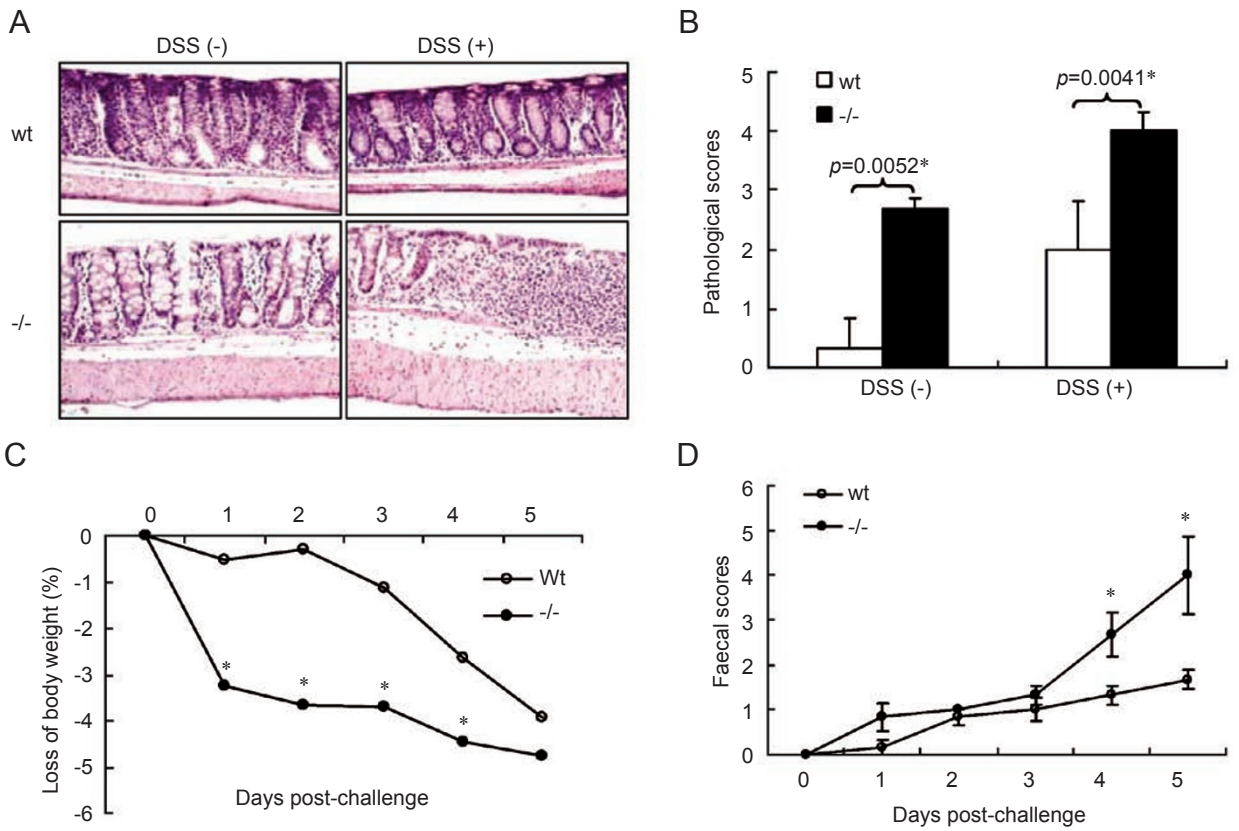

Figure 2 *Rig-I$^{-/-}$* mice exhibit colitis and are susceptible to DSS-induced colitis. **(A)** Histological analysis of colons from wild type and *Rig-I$^{-/-}$* mice with or without treatment with DSS (200×). Wild type and *Rig-I$^{-/-}$* mice of 8 weeks of age were administered with 3% DSS in drinking water. The mice were sacrificed on day 5 and the colons were analyzed. More severe damage and inflammatory infiltration can be observed in the colon mucosa of *Rig-I$^{-/-}$* mice compared with wild-type mice. **(B)** Histological score of colitis in wild type and *Rig-I$^{-/-}$* mice. **(C)** The body weights of the wild type and *Rig-I$^{-/-}$* mice were monitored everyday. The values for body weight are expressed as a percentage of body weight on day 0. Asterisks indicate significant differences between groups ($p < 0.05$). **(D)** Diarrhea in wild type and *Rig-I$^{-/-}$* mice upon treatment with DSS was monitored everyday. Asterisks indicate significant differences between groups ($p < 0.05$). Five mice were used for each group.

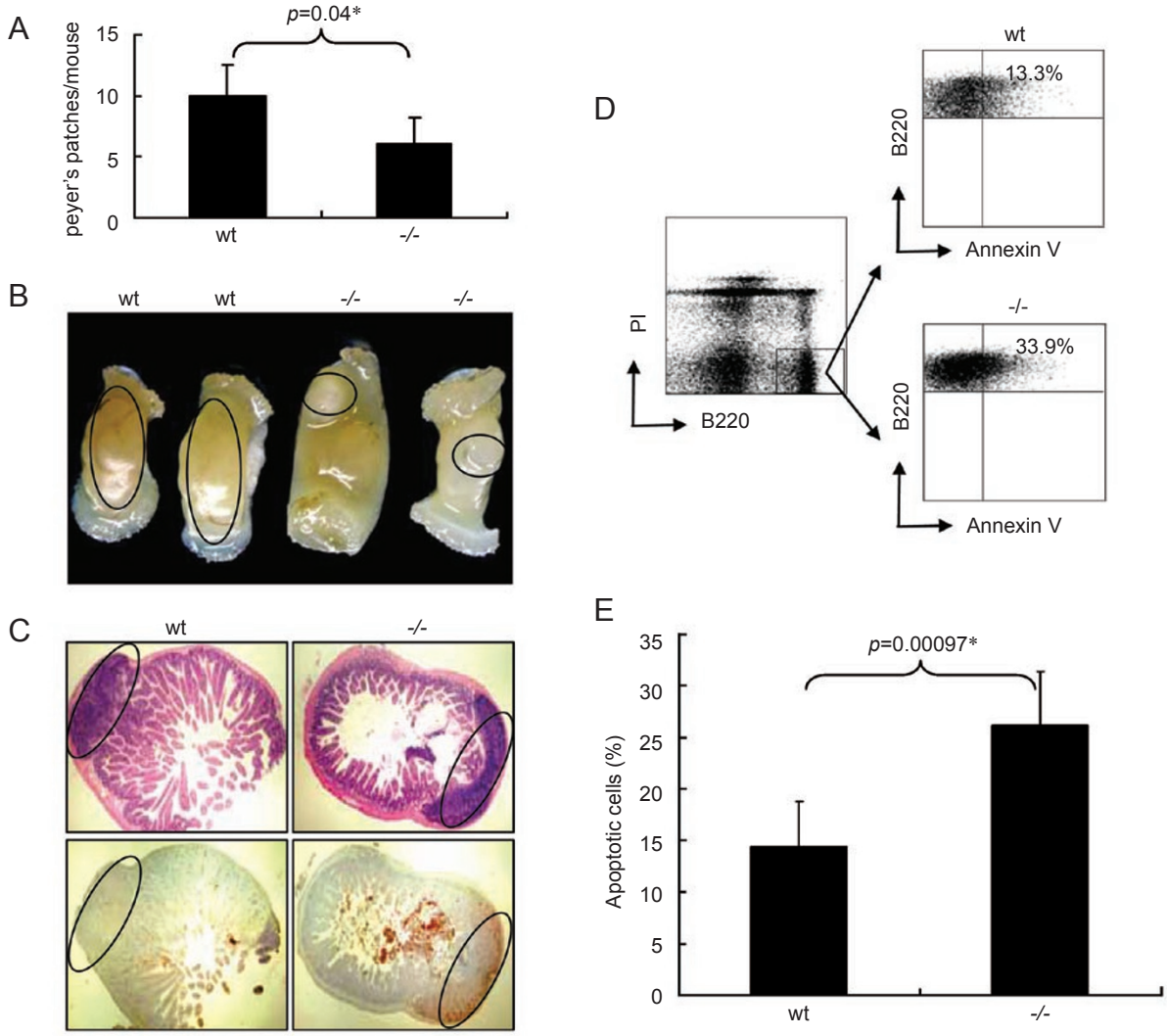

Figure 3 Regression of Peyer's patches in *Rig-I*$^{-/-}$ mice. **(A)** The number of Peyer's patches decreased sharply in *Rig-I*$^{-/-}$ mice compared with wild-type mice (10 mice per each group). **(B)** The size of Peyer's patches (as indicated by circles) in the intestines of *Rig-I*$^{-/-}$ mice decreased significantly (6×, $n = 10$). **(C)** *In situ* TUNNEL analysis shows increased apoptotic cells in Peyer's patches of *Rig-I*$^{-/-}$ mice (400×). Circles indicate the site of Peyer's patches in the transverse section of intestines. **(D)** Apoptotic cells were analyzed by flow cytometry after annexin V staining. As shown in **(D)** and **(E)**, a dramatic increase in apoptotic cells among the B220^{+} population derived from *Rig-I*$^{-/-}$ Peyer's patches can be observed ($n = 5$).

reduced size and number of Peyer's patches raise the possibility of increased apoptosis in *Rig-I*$^{-/-}$ Peyer's patches. As expected, a significant increase in apoptotic cells was detected by *in situ* TUNNEL (Figure 3C), and was further confirmed by Annexin-V flow cytometry in B220^{+} cells in the Peyer's patches deficient for Rig-I (Figure 3D and 3E).

Abnormal splenic T-cell subsets in Rig-I$^{-/-}$ *mice*

It is known that the development of colitis is associated with abnormal T-cell activation [36,37]. For this reason, we compared the proportion and total number of peripheral T-cell subsets in adult (6–8 weeks of age) *Rig-I*$^{-/-}$mice with wild-type mice. The total numbers of splenic CD4^{+} and CD8^{+} T cells were found to be similar between wild type and *Rig-I*$^{-/-}$ mice (data not shown). However, the naïve T cells defined as CD44^{low}CD62L^{high} were markedly decreased ($p = 0.001$), whereas the percentages of CD44^{high}CD62L^{low} effector T cells ($p = 0.008$) and CD44^{high}CD62L^{high} memory T cells ($p = 0.019$) were significantly increased in the CD4^{+} splenic compartment of

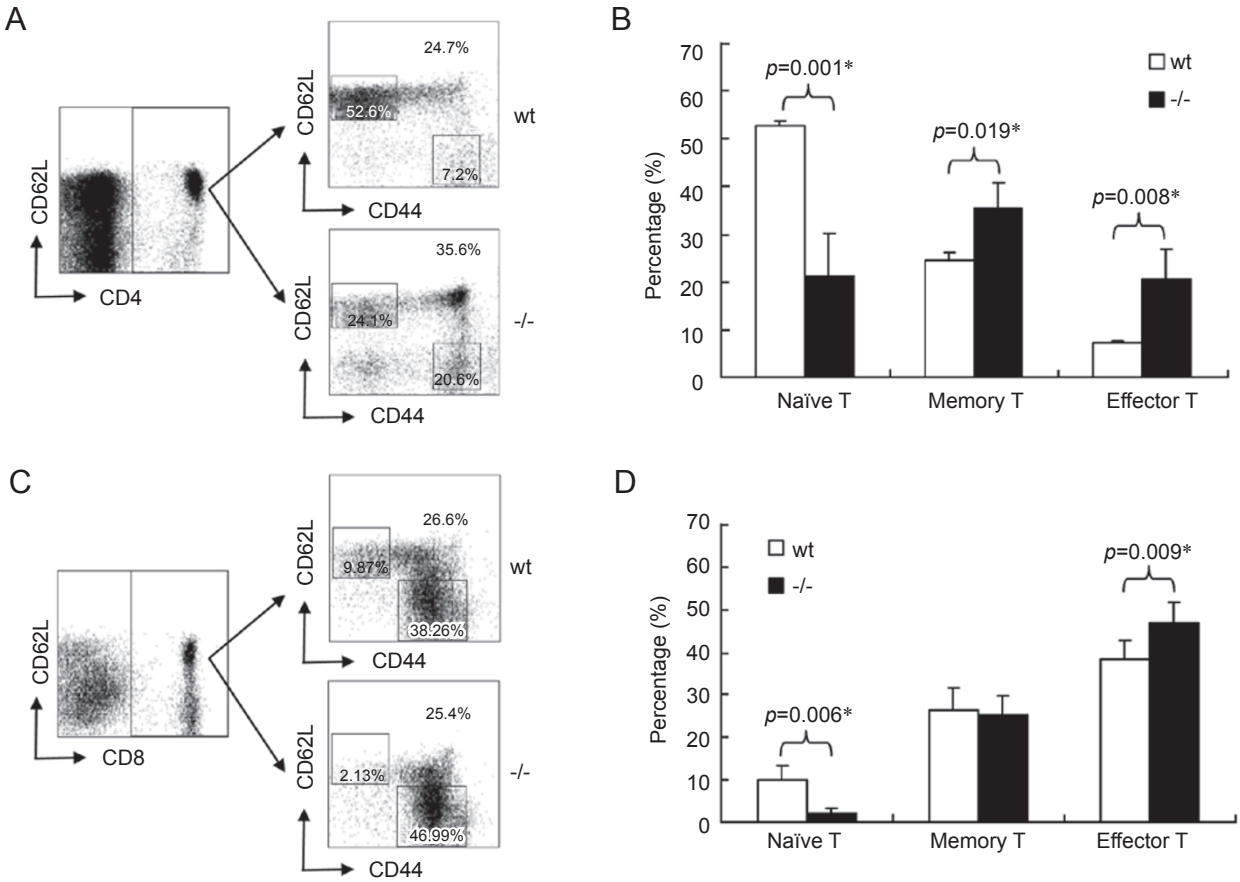

Figure 4 Hyperactivation of peripheral T cells in *Rig-I*$^{-/-}$ mice. Splenocytes from wild type and *Rig-I*$^{-/-}$ mice were stained with CD4, CD8, CD62L and CD44 antibodies conjugated with fluorescence, and the results were analyzed by flow cytometry. To identify naïve T cells (defined as $CD44^{low}CD62L^{high}$), memory T cells (defined as $CD44^{high}CD62L^{high}$) and effector T cells ($CD44^{high}CD62L^{low}$), three-color flow cytometry was performed. **(A, B)** In $CD4^+$ cells, the percentages of memory T cells and effector T cells significantly increased in the absence of Rig-I, while naïve T cells decreased by more than 50% compared with the wild type. The *p*-values that are labeled indicate there are significant differences between groups ($n = 5$). **(C, D)** In $CD8^+$ cells, and in the $CD4^+$ cohort, a marked decrease in naïve T cells and an increase in effector T cells were found. However, memory T cells in $CD8^+$ cells remained unchanged. The data shown are representative of three independent experiments.

Rig-I$^{-/-}$ mice (Figure 4A and 4B). For $CD8^+$ splenic compartments, the percentage of $CD44^{low}CD62L^{high}$ naive T cells was decreased ($p = 0.006$), accompanied by an increased percentage of $CD44^{high}CD62L^{low}$ effector T cells ($p = 0.009$), while $CD44^{high}CD62L^{high}$ memory T cells remained unchanged (Figure 4C and 4D). These findings suggest that the deletion of Rig-I in mice leads to the abnormal activation of peripheral T cells.

Reduced expression of Gαi2 in Rig-I$^{-/-}$ *mice*

Previous data have shown that the induction of colitis in *Gαi2*$^{-/-}$ mice is associated with the regression of Peyer's patches and disorder of T-cell subsets [16]. The phenotype observed in *Rig-I*$^{-/-}$ mice is to some degree similar to that observed in *Gαi2*$^{-/-}$ mice, suggesting that Gαi2 and Rig-I may function in the same signaling pathway in the development of colitis. To address this hypothesis, we first compared Gαi2 expression levels between wild type and *Rig-I*$^{-/-}$ mice. Interestingly, we found that the expression of Gαi2 was significantly reduced in the various tissues tested by real-time PCR (Figure 5A) and western blotting (Figure 5B) in *Rig-I*$^{-/-}$ mice. We then isolated T and B cells from the spleen and checked the difference of *Gαi2* expression between wild type and *Rig-I*$^{-/-}$ cells. At the transcriptional level, it was found that *Gαi2* expression was repressed in both B and T lymphocytes in the absence of Rig-I (Figure 5C and 5D). These data suggest that Rig-I may play a part in the regulation of *Gαi2* expression, and that the develop-

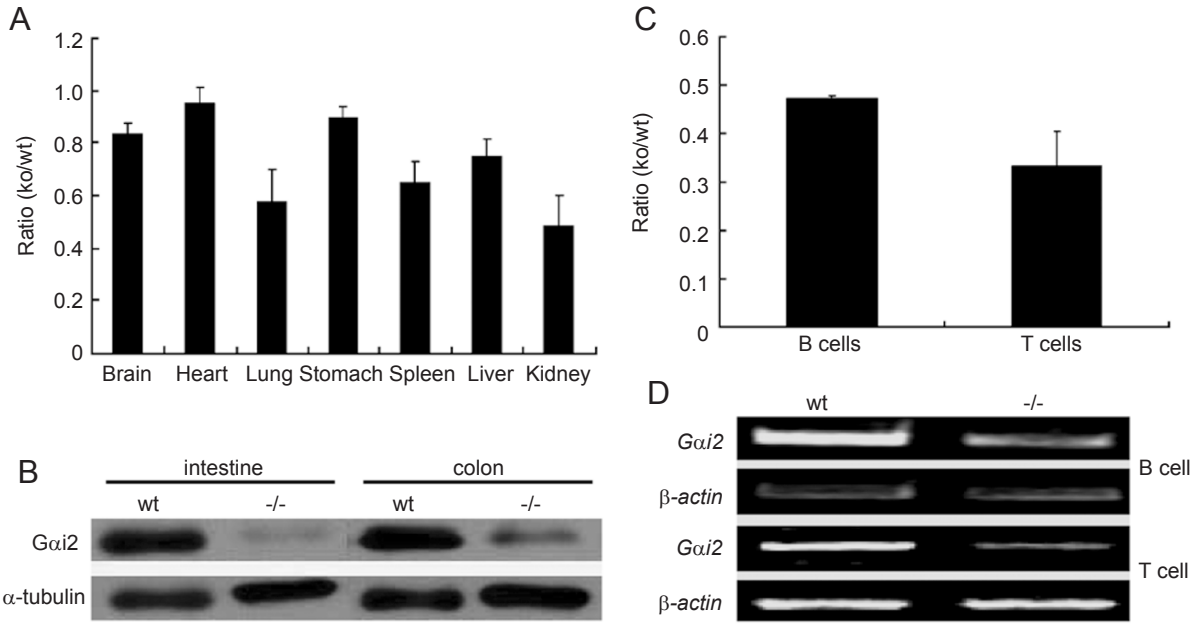

Figure 5 Expression of *Gαi2* is reduced in *Rig-I*$^{-/-}$ tissues or cells. **(A)** Total RNA from the tissues of wild type and *Rig-I*$^{-/-}$ mice was extracted and reversely transcribed to cDNA. The expression of *Gαi2* was analyzed by real-time PCR. The data from real-time PCR were normalized to an internal control and plotted relative to the level of *Gαi2* in the tissues of wild-type mice. Among the tissues tested, *Gαi2* expression was reduced by 30 to 50% in the spleen, lung and kidney, while a mild reduction in the other tissues is shown. **(B)** Western blot analysis shows that *Gαi2* is highly expressed in wild-type intestines and colons. However, *Gαi2* is dramatically reduced in *Rig-I* deficient intestines and colons. α-Tubulin was blotted as a loading control. **(C, D)** The expression of *Gαi2* in sorted T and B lymphocytes was analyzed at the transcriptional level. Splenic T cells were enriched by sorting CD3-PE staining cells. B cells were purified by Dynabeads® Mouse pan B (B220) (Dynal Biotech, Lake Success, NY, USA). Both real-time PCR **(C)** and semi-quantitative RT-PCR **(D)** show decreased expression of *Gαi2* in splenic B and T lymphocytes. β-*actin* in **(D)** serves as an internal control.

ment of colitis and regression of Peyer's patches in *Rig-I*$^{-/-}$ mice may be caused by the downregulation of Gαi2.

Rig-I regulates the transcriptional activity of the Gαi2 promoter

It is well known that Rig-I is induced in NB4 cells by treatment with ATRA [1]. But can the upregulation of endogenous Rig-I by ATRA increase *Gαi2* expression? To this end, we tested the *Gαi2* expression in NB4 cells treated with ATRA. As expected, the induction of Rig-I was paralleled with increased expression of *Gαi2* (Figure 6A), further demonstrating an important role for Rig-I in the regulation of *Gαi2* transcription. To further test the possibility of whether Rig-I regulates *Gαi2* promoter activity, we constructed a *Gαi2* promoter/luciferase reporter construct and co-transfected NIH3T3 cells with increasing doses of the Rig-I expression vector. As shown in Figure 6B, Rig-I indeed activates *Gαi2* promoter activity in a dose-dependent manner. Thus, we may conclude that Rig-I has a crucial role in the normal transcription of *Gαi2*.

Discussion

DExD/H box proteins are putative RNA helicases that are characterized by their ability to unwind dsRNA with intrinsic ATPase activity [38]. They have been implicated in a number of cellular processes that involve the alteration of secondary RNA structures such as translation initiation, nuclear and mitochondrial splicing, and ribosome and spliceosome assembly [39]. *RIG-I* encodes a member of the DExD/H box family proteins. Human *RIG-I* is located on chromosome 9p12 and encodes a 925-amino-acid protein that contains the RNA helicase-DEAD box motif. It is highly conserved from *Caenorhabditis elegans* to mammals and is expressed ubiquitously in the human and mouse. Originally, *RIG-I* was found to be induced in the acute promyelocytic leukemia cell line NB4 during ATRA-induced cell differentiation, suggesting that RIG-I might be an important mediator in the ATRA-signaling pathway [1]. Most importantly, RIG-I was recently identified as an essential regulator for virus-induced antiviral

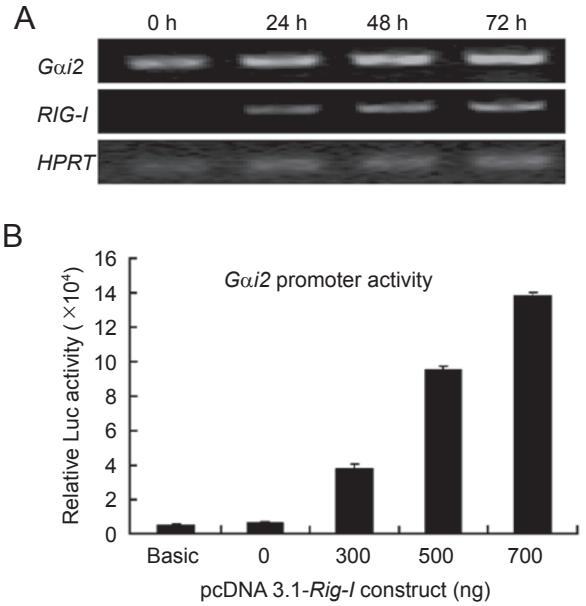

Figure 6 Induction of *Gαi2* promoter activity by Rig-I. **(A)** NB4 cells were treated with 1 μm ATRA for the time indicated, and total RNA was extracted. Induction of *RIG-I* and *Gαi2* expression was analyzed by semi-quantitative RT-PCR. *HPRT* served as a control. The data shown represent one of the three independent experiments. **(B)** NIH3T3 cells were co-transfected with the *Gαi2* promoter luciferase reporter construct, *Renilla* luciferase and pcDNA3.1-*Rig-I* with increasing amounts (0, 300, 500 and 700 ng), or pcDNA3.1. Forty-eight hours after transfection, *Gαi2* promoter-driven luciferase activity was highly activated with increasing amounts of *Rig-I*-expressing vector present. The results shown represent one of three independent experiments.

immunity, capable of sensing intracellular viral dsRNA, which transduces signals through an adaptor protein (MAVS/IPS-1/VISA/Cardif), leading to the activation of IRF-3 and NF-κB, and augmenting interferon production in response to viral infection [4-11]. The *in vivo* importance of Rig-I in antiviral defense was further demonstrated in *Rig-I*-deficient mice, in which exons 8 to 10 of *Rig-I* were deleted, by showing the cell-type-specific requirements for Rig-I in the antiviral response [13]. Unfortunately, *Rig-I* knockout mice generated by Akira's group mostly died during embryogenesis, and a few newborn mice died within 3 weeks after birth owing to extensive apoptosis in the fetal liver. In this study, we also generated *Rig-I* knockout mice, in which 5 exons (exons 4 to 8) encoding part of CARD domain 2, and the A and B motifs of the RNA helicase domain (aa141-405) were replaced with a *Neo* cassette by homologous recombination. Disruption of Rig-I was demonstrated by northern blot analysis using the 3′-end fragment of *Rig-I* cDNA (477 bp, composed of exons 11 to 14) as a probe, and by western blot analysis using the polyclonal antibody specific to RIG-I. Unlike the previous study [13], our homozygous *Rig-I* knockout mice were viable and fertile. The genotype distribution in the littermates obtained from crossing heterozygote mice follows a Mendelian pattern of inheritance. MEFs derived from our *Rig-I*$^{-/-}$ mice also showed a compromised antiviral response, similar to the previous report (unpublished data). However, the *Rig-I*$^{-/-}$ mice displayed significant age-dependent loss of body weight. Extensive pathological analysis showed that 70% of adult *Rig-I*$^{-/-}$ mice spontaneously developed a colitis-like phenotype with increased susceptibility to DSS-induced colitis. The different outcomes between our mutant mice and that reported by Kato *et al*. [13] likely result from the disruption of different regions of the *Rig-I* gene. In fact, this kind of phenomenon is not uncommon in mouse mutagenesis studies. A typical example emerged from the comparison of the phenotypes represented by three different *Prnp*$^{-/-}$ mice [40]. This could be explained by the different truncated proteins that are expressed after genomic modification, although they may be expressed at very low levels. In our case, this possibility could not be excluded, but northern or western blotting detected no signals that correspond to truncated Rig-I messages or proteins. The *Rig-I*$^{-/-}$ mice we generated survived and displayed a colitis-like phenotype, providing us an alternative model for studying the mechanisms that underlie inflammatory bowel disease, including colitis.

Inflammatory bowel disease is considered to be associated with a breakdown of tolerance to the resident intestinal flora [41, 42] and immune activation in the gut-associated lymphatic tissue (GALT). The GALT consists of Peyer's patches and mesenteric lymph nodes as organized intestinal lymphoid follicles. Previous studies have shown that a deficiency of Peyer's patches and mesenteric lymph nodes may be in part responsible for the development of colitis in mice. It is known that intraluminal and intestinal wall antigens have the capacity to induce tolerance toward inflammatory intestinal immune responses. A reduction in the number of Peyer's patches and mesenteric lymph nodes, especially the loss of normally present regulatory cells (such as dendritic cells) in these organs, may result in the failure of tolerance induction in the gut [43]. Therefore, the decrease in Peyer's patches that is due to increased apoptosis is, to some degree, related to the induction of colitis in *Rig-I*$^{-/-}$ mice.

It has been shown that the disruption of several genes in mice leads to chronic inflammation of the bowel [17, 44-46]. Among them, Gai2-deficienct mice display growth retardation and develop lethal diffuse colitis with clinical and histopathological features that closely resemble ulcerative colitis in humans [17]. It has also been shown that

Gαi2$^{-/-}$ mice exhibit a local increase in memory CD4$^+$ and CD8$^+$ cells that are characterized by increased levels of CD44 and decreased levels of CD45RB and CD62L, an increase in pro-inflammatory Th1-type cytokines and an increase in the infiltration of activated CD4$^+$ T cells in the intestinal mucosa [47, 48]. All of these findings strongly suggest that Gαi2-deficiency leads to a hyperimmune response and that the Gαi2 protein may negatively regulate T-cell immunity [17, 24, 47].

The regression of Peyer's patches and development of colitis in *Rig-I*$^{-/-}$ mice raise the possibility that Rig-I may play a part in the regulation of T-cell homeostasis. As expected, we found that Rig-I deficiency leads to an increase in splenic CD4$^+$ and CD8$^+$ effector T cells with a decrease of naïve T cells, indicating the hyper-activation of effector T cells in *Rig-I*$^{-/-}$ mice. These data also suggest an important role for Rig-I in the regulation of T-cell activation.

Gαi2$^{-/-}$ mice display colitis with 100% penetrance with smaller Peyer's patches and *Gαi2*$^{-/-}$ mice also exhibit disorders of the T-cell subsets [16]. These observations suggest that there may be a link between Rig-I and Gαi2. Therefore, we examined Gαi2 expression in various tissues of wild type and *Rig-I*$^{-/-}$ mice. As expected, *Gαi2* expression decreased distinctly in many tissues of *Rig-I*$^{-/-}$ mice, especially in the colons and intestines. On the contrary, up-regulation of Rig-I in NB4 cells upon treatment with ATRA is accompanied by elevated *Gαi2* expression. Luciferase assay further demonstrated that Rig-I can markedly activate *Gαi2* promoter activity in a dose-dependent manner. Based on these findings, we propose that Rig-I may function as a positive regulator for *Gαi2* transcription.

In this report, we identified a novel role of Rig-I in T-cell activation and *Gαi2* expression by showing the distinct phenotypes of *Rig-I*$^{-/-}$ mice. The development of colitis in *Rig-I*$^{-/-}$ mice might be in part associated with the downregulation of *Gαi2* and disturbed T-cell homeostasis.

Acknowledgments

This work was partially supported by grants from the National Natural Science Foundation of China (39925023), Ministry of Science and Technology (2001CB509901, 2001AA216081), Ministry of Education (00TPJS111) of China, Science and Technology Commission of Shanghai Municipality (03DZ14088, 06DZ05907), E-Institutes of Shanghai Municipal Education Commission (E03003), and Foundation of Shanghai Jiao Tong University and School of Medicine (BXJ0604, 2004JY05). We thank Professor Bao-xue Ge for providing Rig-I polyclonal antibody. We are also grateful to co-workers in the laboratory for helpful discussions.

References

1 Sun YW. RIG-I, a human homolog gene of RNA helicase, is induced by retinoic acid during the differentiation of acute promyelocytic leukemia cells. Thesis, Shanghai Second Medical University, 1997.
2 Liu TX, Zhang JW, Tao J, *et al*. Gene expression networks underlying retinoic acid-induced differentiation of acute promyelocytic leukemia cells. Blood 2000; **96**:1496-1504.
3 Johnson CL, Gale M Jr. CARD games between virus and host get a new player. Trends Immunol 2006; **27**:1-4.
4 Imaizumi T, Hatakeyama M, Yamashita K, *et al*. Double-stranded RNA induces the synthesis of retinoic acid-inducible gene-I in vascular endothelial cells. Endothelium 2005; **12**:133-137.
5 Huang J, Liu T, Xu LG, *et al*. SIKE is an IKK epsilon/TBK1-associated suppressor of TLR3- and virus-triggered IRF-3 activation pathways. EMBO J 2005; **24**:4018-4028.
6 Melchjorsen J, Jensen SB, Malmgaard L, *et al*. Activation of innate defense against a paramyxovirus is mediated by RIG-I and TLR7 and TLR8 in a cell-type-specific manner. J Virol 2005; **79**:12944-12951.
7 Fensterl V, Grotheer D, Berk I, *et al*. Hepatitis A virus suppresses RIG-I-mediated IRF-3 activation to block induction of beta interferon. J Virol 2005; **79**:10968-10977.
8 Meylan E, Curran J, Hofmann K, *et al*. Cardif is an adaptor protein in the RIG-I antiviral pathway and is targeted by hepatitis C virus. Nature 2005; **437**:1167-1172.
9 Seth RB, Sun L, Ea CK, *et al*. Identification and characterization of MAVS, a mitochondrial antiviral signaling protein that activates NF-kappaB and IRF 3. Cell 2005; **122**:669-682.
10 Kawai T, Takahashi K, Sato S, *et al*. IPS-1, an adaptor triggering RIG-I- and Mda5-mediated type I interferon induction. Nat Immunol 2005; **6**:981-988.
11 Xu LG, Wang YY, Han KJ, *et al*. VISA is an adapter protein required for virus-triggered IFN-beta signaling. Mol Cell 2005; **19**:727-740.
12 Lin R, Yang L, Nakhaei P, *et al*. Negative regulation of the retinoic acid-inducible gene I-induced antiviral state by the ubiquitin-editing protein A20. J Biol Chem 2006; **281**:2095-2103.
13 Kato H, Sato S, Yoneyama M, *et al*. Cell type-specific involvement of RIG-I in antiviral response. Immunity 2005; **23**:19-28.
14 Cui XF, Imaizumi T, Yoshida H, *et al*. Retinoic acid-inducible gene-I is induced by interferon-gamma and regulates the expression of interferon-gamma stimulated gene 15 in MCF-7 cells. Biochem Cell Biol 2004; **82**:401-405.
15 Imaizumi T, Aratani S, Nakajima T, *et al*. Retinoic acid-inducible gene-I is induced in endothelial cells by LPS and regulates expression of COX-2. Biochem Biophys Res Commun 2002; **292**:274-279.
16 Ohman L, Franzen L, Rudolph U, *et al*. Regression of Peyer's patches in G alpha i2 deficient mice prior to colitis is associated with reduced expression of Bcl-2 and increased apoptosis. Gut 2002; **51**:392-397.
17 Rudolph U, Finegold MJ, Rich SS, *et al*. Ulcerative colitis and adenocarcinoma of the colon in G alpha i2-deficient mice. Nat Genet 1995; **10**:143-150.
18 Hampe J, Lynch NJ, Daniels S, *et al*. Fine mapping of the chromosome 3p susceptibility locus in inflammatory bowel disease. Gut 2001; **48**:191-197.

19 Arinze IJ, Kawai Y. Transcriptional activation of the human Galphai2 gene promoter through nuclear factor-kappaB and antioxidant response elements. J Biol Chem 2005; **280**:9786-9795.
20 Saha C, Nigam SK, Denker BM. Involvement of Galphai2 in the maintenance and biogenesis of epithelial cell tight junctions. J Biol Chem 1998; **273**:21629-21633.
21 Holstein DM, Berg KA, Leeb-Lundberg LM, *et al*. Calcium-sensing receptor-mediated ERK1/2 activation requires Galphai2 coupling and dynamin-independent receptor internalization. J Biol Chem 2004;**279**:10060-10069.
22 Goel R, Phillips-Mason PJ, Gardner A. Alpha-thrombin-mediated phosphatidylinositol 3-kinase activation through release of Gbetagamma dimers from Galphaq and Galphai2. J Biol Chem 2004; **279**:6701-6710.
23 Dalwadi H, Wei B, Schrage M, *et al*. B cell developmental requirement for the G alpha i2 gene. J Immunol 2003; **170**:1707-1715.
24 Huang TT, Zong Y, Dalwadi H, *et al*. TCR-mediated hyperresponsiveness of autoimmune Galphai2-$^{/-}$ mice is an intrinsic naive CD4(+) T cell disorder selective for the Galphai2 subunit. Int Immunol 2003; **15**:1359-1367.
25 Zhang Y, Finegold MJ, Jin Y, *et al*. Accelerated transition from the double-positive to single-positive thymocytes in G alpha i2-deficient mice. Int Immunol 2005; **17**:233-243.
26 Castagliuolo I, Morteau O, Keates AC, *et al*. Protective effects of neurokinin-1 receptor during colitis in mice: role of the epidermal growth factor receptor. Br J Pharmacol 2002; **136**:271-279.
27 Strober W, Fuss IJ, Blumberg RS. The immunology of mucosal models of inflammation. Annu Rev Immunol 2002; **20**:495-549.
28 Okayasu I, Hatakeyama S, Yamada M, *et al*. A novel method in the induction of reliable experimental acute and chronic ulcerative colitis in mice. Gastroenterology 1990; **98**:694-702.
29 Yoshihara K, Yajima T, Kubo C, Yoshikai Y. Role of interleukin 15 in colitis induced by dextran sulphate sodium in mice. Gut 2006; **55**:334-341.
30 Beck PL, Rosenberg IM, Xavier RJ, *et al*. Transforming growth factor beta mediates intestinal healing and susceptibility to injury in vitro and in vivothrough epithelial cells. Am J Pathol 2003; **162**:597-608.
31 Opitz B, Vinzing M, van Laak V, *et al*. Legionella pneumophila induces IFNbeta in lung epithelial cells via IPS-1 and IRF3, which also control bacterial replication. J Biol Chem 2006; **281**:36173-36179.
32 Yoneyama M, Kikuchi M, Matsumoto K, *et al*. Shared and unique functions of the DExD/H-box helicases RIG-I, MDA5, and LGP2 in antiviral innate immunity. J Immunol 2005; **175**:2851-2858.
33 Lin R, Lacoste J, Nakhaei P, *et al*. Dissociation of a MAVS/IPS-1/VISA/Cardif-IKKepsilon molecular complex from the mitochondrial outer membrane by hepatitis C virus NS3-4A proteolytic cleavage. J Virol 2006; **80**:6072-6083.
34 Pichlmair A, Schulz O, Tan CP, *et al*. RIG-I-mediated antiviral responses to single-stranded RNA bearing 5′-phosphates. Science 2006; **314**:997-1001.
35 Gitlin L, Barchet W, Gilfillan S, *et al*. Essential role of mda-5 in type I IFN responses to polyriboinosinic:polyribocytidylic acid and encephalomyocarditis picornavirus. Proc Natl Acad Sci USA 2006; **103**:8459-8464.
36 Martins GA, Cimmino L, Shapiro-Shelef M, *et al*. Transcriptional repressor Blimp-1 regulates T cell homeostasis and function. Nat Immunol 2006; **7**:457-465.
37 Kallies A, Hawkins ED, Belz GT, *et al*. Transcriptional repressor Blimp-1 is essential for T cell homeostasis and self-tolerance. Nat Immunol 2006; **7**:466-474.
38 Rocak S, Emery B, Tanner NK, Linder P. Characterization of the ATPase and unwinding activities of the yeast DEAD-box protein Has1p and the analysis of the roles of the conserved motifs. Nucleic Acids Res 2005; **33**:999-1009.
39 de la Cruz J, Kressler D, Linder P. Unwinding RNA in Saccharomyces cerevisiae: DEAD-box proteins and related families. Trends Biochem. Sci 1999; **24**:192-198.
40 Weissmann C, Aguzzi A. Perspectives: neurobiology. PrP's double causes trouble. Science 1999; **286**:914-915.
41 Duchmann R, Kaiser I, Hermann E, Mayet W, Ewe K, Meyer zumBuschenfelde KH. Tolerance exists towards resident intestinal flora but is broken in active inflammatory bowel disease (IBD). Clin Exp Immunol 1995; **102**:448-455.
42 Duchmann R, Schmitt E, Knolle P, Meyer zum Buschenfelde KH, Neurath M. Tolerance towards resident intestinal flora in mice is abrogated in experimental colitis and restored by treatment with interleukin-10 or antibodies to interleukin-12. Eur J Immunol 1996; **26**:934-938.
43 Thomas W Spahn, Hermann Herbst, Paul D Rennert, *et al*. Induction of colitis in mice deficient of Peyer's patches and mesenteric lymph nodes is associated with increased disease severity and formation of colonic lymphoid patches. Am J Pathol 2002; **161**:2273-2282.
44 Ehrhardt RO, Ludviksson BR, Gray B, Neurath M, Strober W. Induction and prevention of colonic inflammation in IL-2-deficient mice. J Immunol 1997; **158**:566-573.
45 Kühn R, Löhler J, Rennick D, Rajewsky K, Müller W. Interleukin-10-deficient mice develop chronic enterocolitis. Cell 1993; **75**:263-274.
46 Mombaerts P, Mizoguchi E, Grusby MJ, Glimcher LH, Bhan AK, Tonegawa S. Spontaneous development of inflammatory bowel disease in T cell receptor mutant mice. Cell 1993; **75**:275-282.
47 Ohman L, Franzen L, Rudolph U, Harriman GR, Hultgren HE. Immune activation in the intestinal mucosa before the onset of colitis in Galphai2-deficient mice. Scand J Immunol 2000; **52**:80.
48 Hornquist CE, Lu X, Rogers-Fani PM, *et al*. G(alpha)i2-deficient mice with colitis exhibit a local increase in memory CD4^{+} T cells and proinflammatory Th1-type cytokines. J Immunol 1997; **158**:1068.